Nuclear Inst. and Methods in Physics Research, A 1046 (2023) 167711

Contents lists available at ScienceDirect

Nuclear Inst. and Methods in Physics Research, A

journal homepage: www.elsevier.com/locate/nima

Technical Notes

Application of adaptive filtering algorithm to the stability problem for double crystal monochromator. Part II: Hybrid algorithms

Yang Bai [a,b], Xuepeng Gong [a,*], Qipeng Lu [a], Yuan Song [a], Wanqian Zhu [c], Song Xue [c], Dazhuang Wang [a], Zhongqi Peng [a], Zhen Zhang [a]

[a] Changchun Institute of Optics, Fine Mechanics and Physics, Chinese Academy of Sciences, Changchun 130033, China
[b] University of Chinese Academy of Sciences, Beijing 100049, China
[c] Shanghai Advanced Research Institute, Chinese Academy of Sciences, Shanghai 201204, China

ARTICLE INFO

Keywords:
Synchrotron radiation sources
Double crystal monochromator
Adaptive filtering algorithms
Hybrid algorithms
Active vibration control

ABSTRACT

The beam line energy of X-ray beams from synchrotron radiation sources is increasing dramatically, which puts higher demands on the stability of double crystal monochromator (DCM). In this paper, the vibration suppression performance of FxLMS-P, FxLMS-PI, and FxLMS-PID hybrid algorithms are presented under Bragg@12.66KeV and Bragg@9KeV operating conditions for the measured vibration signals of DCM at SSRF (Shanghai Synchrotron Radiation Facility). Moreover, the unknown disturbance rejection performance of FxNLMS-P, FxNLMS-PI, and FxNLMS-PID hybrid algorithms is demonstrated under Bragg@5KeV operating conditions for the measured vibration signals of DCM at SSRF. The results show that the FxLMS-P, FxLMS-PI, and FxLMS-PID hybrid algorithms provide excellent vibration suppression under Bragg@9KeV operating conditions; Conversely, the FxLMS-PID hybrid algorithm vibration suppression capability was disabled under Bragg@12KeV operating conditions. In particular, the FxLMS-based hybrid algorithm lacks vibration rejection efficiency under Bragg@5KeV operating conditions, which is perfectly solved by the FxNLMS-based hybrid algorithm.

1. Introduction

The new generation synchrotron light sources are mainly developed toward two directions: X-ray free electron laser devices and diffraction-limited storage ring light sources. In recent years, several countries around the world have started to design and build diffraction-limited storage ring devices, including the completed MAX-IV laboratory in Sweden, the Sirius Light Source in Brazil under construction, the APS-U Light Source in the United States, and the High Energy Synchrotron Radiation Light Source in China [1–5]. The development of synchrotron light sources based on biology, chemistry, physics, advanced manufacturing and other fields [6–9]; the light source performance put forward higher requirements. The stability index of DCM is the key index of X-ray beamline of synchrotron radiation source. Synchrotron radiation laboratories worldwide mainly use optimization of cooling tube, improvement of crystal clamping mechanism and application of damping materials to enhance the stability of DCM [10–15].

Adaptive filtering algorithms are widely applied in the field of active control vibration. Haraguchi et al. [17] used the FxLMS (Filter-x Least Mean Square) algorithm and finite impulse response filter to effectively solve the control system instability problem caused by the presence of secondary paths, which became one of the most classical and widely used algorithms in active vibration control research. Guan and Teik C. Lim and Mingfeng Li proposed an active control method for gearbox vibration using an FxLMS control algorithm with amplification delay to generate a suitable control signal for the piezoelectric stack actuator to produce a control force so as to suppress the vibration of the gear pair caused by the gear transmission error excitation [18–23]; Kwong [24], Mathew [25], Aboulnasr [26], Pazaitis [27], Mader [28], WeePeng [29], Shin [30], et al. proposed some typical variable-step LMS algorithms; Eriksson [31] first proposed a FuLMS (Filter-u Least Mean Square) method for active noise control; Mayyas [32] proposed a variable-step selective local update least mean square algorithm, which has lower computational complexity compared to the LMS algorithm; Dariusz Bismor [33] proposed the PU-LMS (Partial Update LMS) algorithm, which optimizes some parameters and improves the performance of the control system; Ho-Wuk Kim [34] et al. optimized the FuLMS (Filter-u Least Mean Square) algorithm and applied it to active noise control to solve the problem of shorter pipeline noise; Lingbo Xie et al. optimized the FuLMS algorithm and applied it to the active vibration control of flexible clamping plates [35]. Amrita Puri [36] et al. proposed a model-based FxLMS algorithm applied to the control of acoustic-vibration lines, the basic block diagram of the algorithm is

* Corresponding author.
E-mail addresses: gongxuepeng120@foxmail.com (X. Gong), luqipeng@126.com (Q. Lu).

https://doi.org/10.1016/j.nima.2022.167711
Received 24 August 2022; Received in revised form 17 October 2022; Accepted 23 October 2022
Available online 4 November 2022
0168-9002/

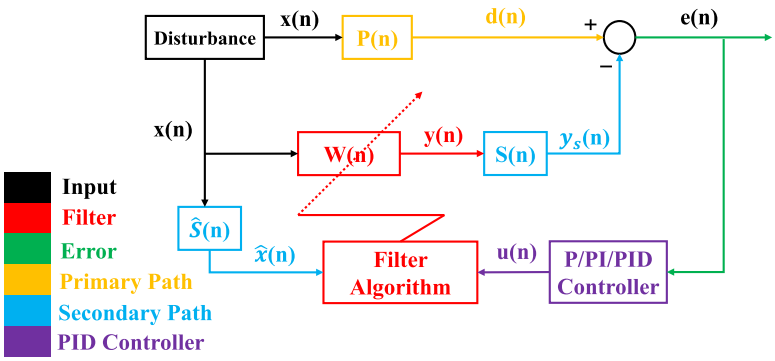

Fig. 1. The block diagram of hybrid algorithm filtering algorithm.

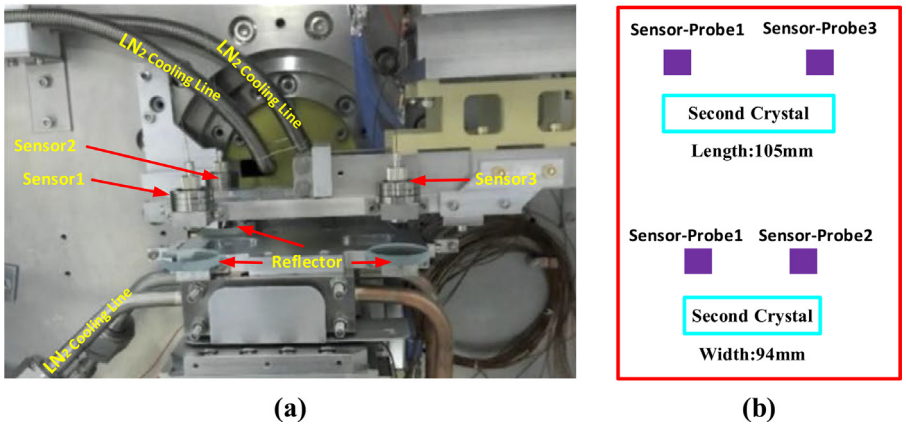

Fig. 2. Test diagram. (a) Actual measurement map [16]. (b) Test schematic.

shown in Fig. 13; Philipp Zech et al. applied the exact phase and narrow bandwidth adaptive algorithm without the second channel model [37] to solve the gearbox vibration problem; Y.S. Wang [38] et al. applied the FxLMS algorithm based on discrete wavelet transform optimized FxLMS algorithm to solve vibration control problems in the automotive domain; Lei Luo [39] et al. applied the leaked FxNLMS algorithm to nonlinear systems.

In this paper, the vibration suppression performance of hybrid algorithms (mainly FxLMS-P, FxLMS-PI, FxLMS-PID) are verified based on the measured vibration signals of DCM under Bragg@12.66KeV and Bragg@9KeV operating conditions at SSRF. On the other hand, the vibration suppression performance of the hybrid algorithm(mainly FxNLMS-P, FxNLMS-PI, FxNLMS-PID) is validated based on the measured vibration signals of DCM under Bragg@5KeV operating conditions. The results show that the FxLMS-P, FxLMS-PI, and FxLMS-PID hybrid algorithms provide excellent vibration suppression under Bragg@9KeV operating conditions, which angular displacement is limited to less than 1 nrad. Conversely, the FxLMS-PID hybrid algorithm vibration suppression capability was disabled under Bragg@12KeV operating conditions. In particular, the FxLMS-based hybrid algorithm lacks vibration rejection efficiency under Bragg@5KeV operating conditions, which is perfectly solved by the FxNLMS-based hybrid algorithm, and FxNLMS-based hybrid algorithm suppresses the effect of unknown perturbations on DCM effectively.

2. Hybrid algorithms

In general, it can improve the vibration suppression performance and convergence accuracy by combining the typical FxLMS algorithm and PID (P/PI) algorithm together. The block diagram of a typical adaptive filtering algorithm is shown in Fig. 1.

The expected signal is

$$d(n) = X(n) * P(n) \tag{1}$$

The anti-vibration signal is

$$y_s(n) = y(n) * S(n) \tag{2}$$

The output signal (filtered signal) of the secondary channel is

$$\hat{X}(n) = W(n) * \hat{S}(n) \tag{3}$$

The residual error signal is

$$e(n) = d(n) - y_s(n) = X(n) * P(n) - y(n) * S(n) \tag{4}$$

The gradient vector is zero when the filter power coefficients reach to be the optimal solution.

$$W(n+1) = W(n) + 2\mu u(n)\hat{X}(n) \tag{5}$$

The $u(n)$ is

$$u(n) = K_P \cdot e(n) + K_I \cdot \frac{1}{S} + K_D \frac{N}{1 + N \cdot T_s \frac{1}{z-1}} \cdot e(n) \tag{6}$$

3. Case verification

The vibration test device was constructed to obtain the vibration signals of different working conditions of the double crystal monochromator in Shanghai synchrotron radiation facility (SSRF), and the actual test diagram is shown in Fig. 2. Elimination of the trend term (sensor offset) is performed by the sgolayfilt filtering algorithm. The vibration test results under Bragg@12.66KeV Bragg@9KeV working conditions are shown in Fig. 3; the vibration test results under Bragg@5KeV are shown in Fig. 4.

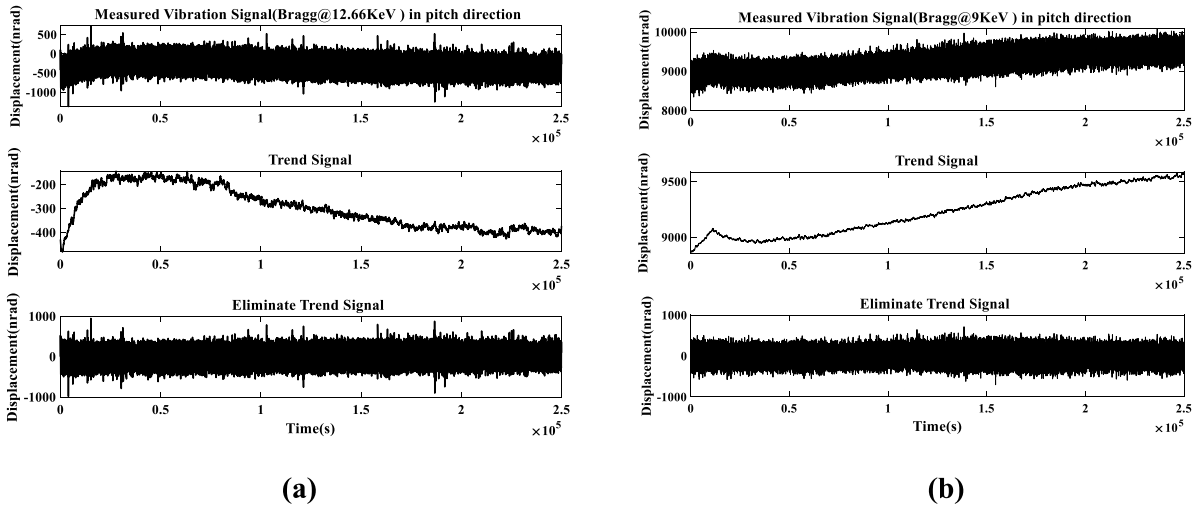

Fig. 3. Test results. (a) Bragg@12.66KeV. (b) Bragg@9KeV.

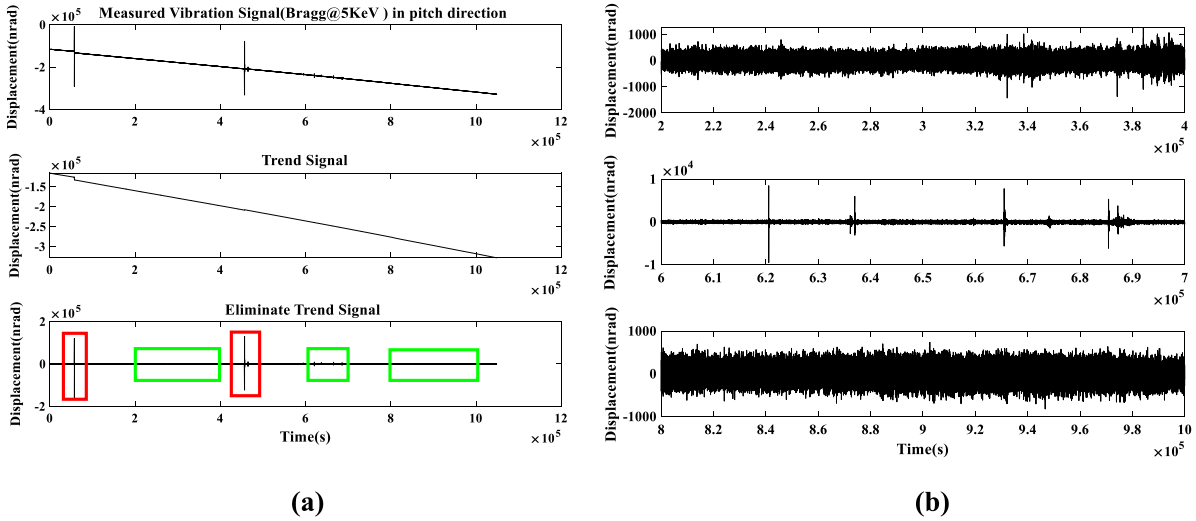

Fig. 4. Test results. (a) Bragg@5KeV. (b) Green wireframe amplifies the signal.

3.1. Case 1: Bragg@12.66KeV

Measured vibration signals from DCM under Bragg@12.66KeV conditions are applied to verify the accuracy of FxLMS-P, FxLMS-PI, FxLMS-PID algorithms. The vibration suppression time-domain, frequency-domain results, vibration level results and weight iteration results of FxLMS-P, FxLMS-PI, FxLMS-PID algorithms are shown in Figs. 5–7 as follows.

As shown from the time-domain results in Fig. 5(a), the FxLMS-P hybrid algorithm decreases the Pitch direction displacement by about 94.14%; however, the green wireframe in Fig. 5(a) shows that the Pitch direction displacement signal is abnormally amplified, which is not allowed during the actual operation of the DCM. From the frequency-domain results in Fig. 5(b) and the vibration level results in Fig. 5(c), it is seen that the FxLMS-P hybrid algorithm has excellent vibration suppression performance. Similarly, it can be seen from Fig. 6(a), Fig. 6(b), Fig. 6(c) and Fig. 6(d) that the FxLMS-PI hybrid algorithm vibration suppression is significant which reduces the angular displacement in the Pitch direction by about 99.38%. In particular, the FxLMS-PI algorithm effectively avoids the problem in Fig. 5(a) that appears in the FxLMS-P hybrid algorithm. From Fig. 7(a), Fig. 7(b), Fig. 7(c) and Fig. 7(d), it can be seen that the FxLMS-PID hybrid algorithm completely invalidates under Bragg@12.66KeV conditions. The differential link in the PID algorithm can accelerate the system dynamic response, however, in a practical discrete control system, the differential link tends to amplify the noise.

3.2. Case 2: Bragg@9KeV

In this case, the measured vibration signals from DCM under Bragg@9KeV conditions are taken to validate the accuracy of FxLMS-P, FxLMS-PI and FxLMS-PID algorithms. The results of FxLMS-P, FxLMS-PI and FxLMS-PID algorithms are shown in Figs. 8–10 as follows.

From the time domain-results of Fig. 8(a), Fig. 9(a) and Fig. 10(a), it is known that the FxLMS-P, FxLMS-PI and FxLMS-PID algorithms decrease the angular displacement by about 99.51%, 99.46%, 99.52% as respectively, and can keep the angular displacement below 1 nrad; From the frequency-domain results of Fig. 8(b), Fig. 9(b) and Fig. 10(b) and the vibration level results of Fig. 8(c), Fig. 9(c) and Fig. 10(c), the vibration suppression effect is perfectly significant. From the results of the weight iterations in Fig. 8(d), Fig. 9(d) and Fig. 10(d), it is known that the FxLMS-P, FxLMS-PI and FxLMS-PID hybrid algorithms converge faster and the weight iterations more stable.

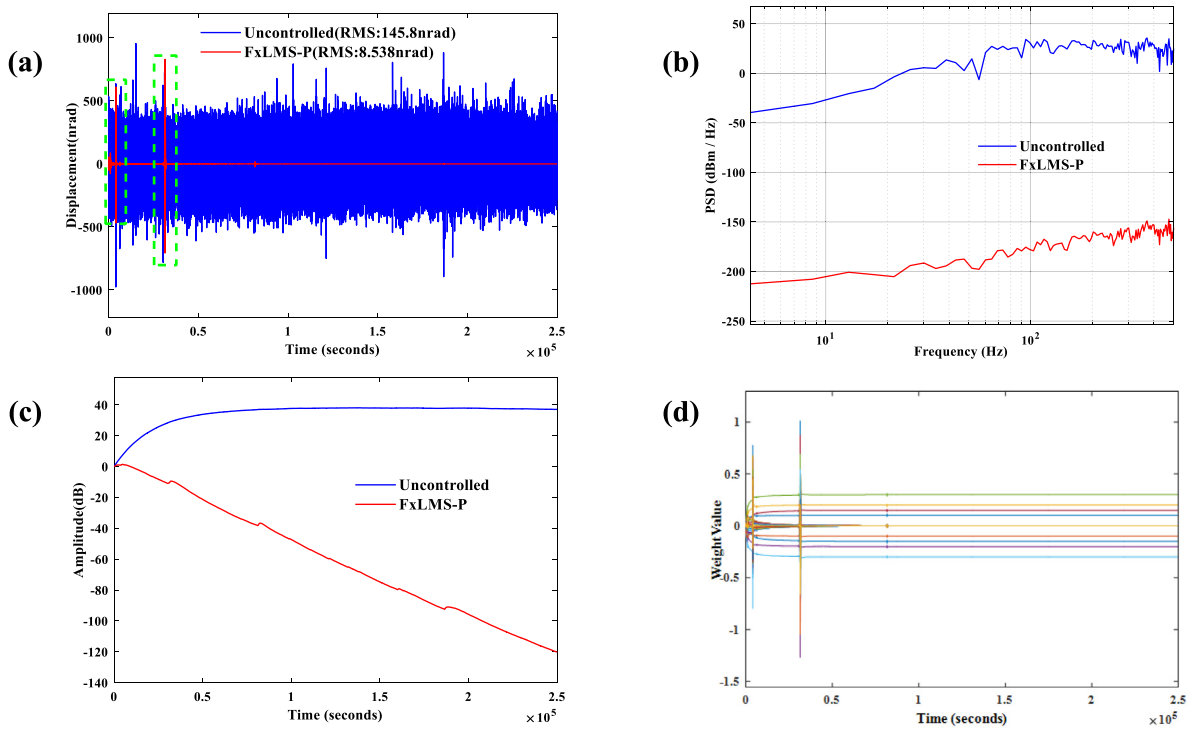

Fig. 5. FxLMS-P algorithm vibration suppression results. (a) Time-domain results (b) Frequency-domain results (c) Vibration level results (d) Weight iteration results.

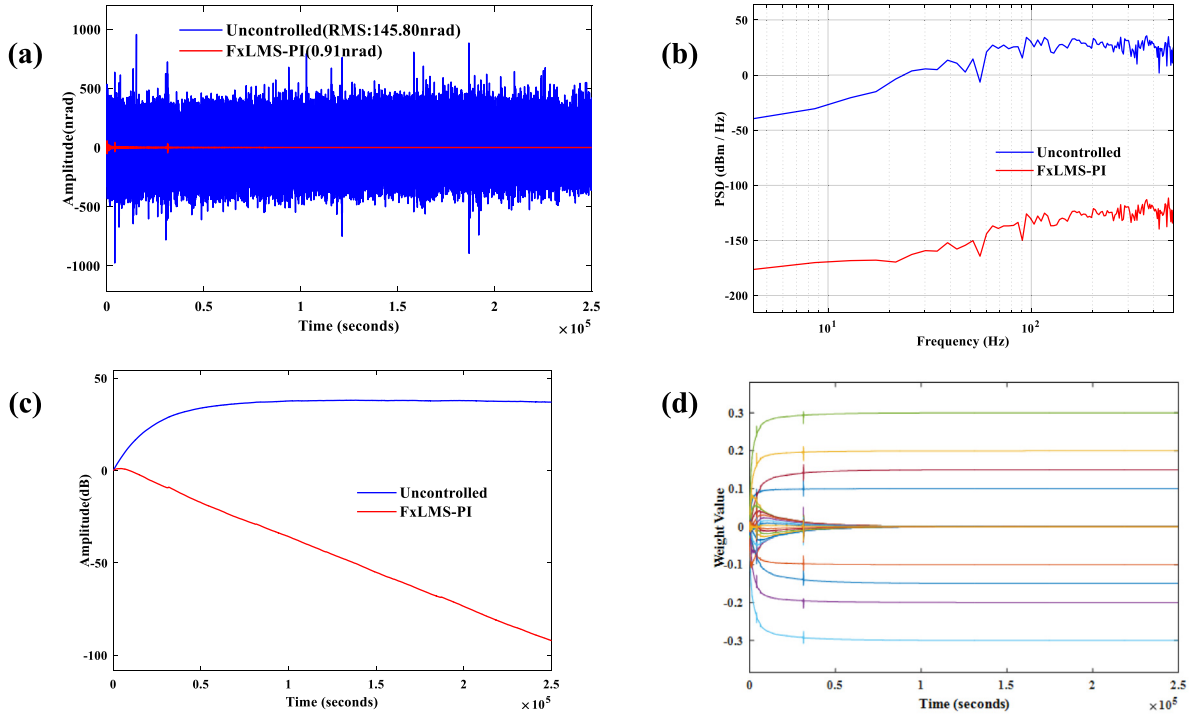

Fig. 6. FxLMS-PI algorithm vibration suppression results. (a) Time-domain results (b) Frequency-domain results (c) Vibration level results (d) Weight iteration results.

3.3. Case 3: Bragg@5KeV

From the results of the measured vibration signal in Fig. 4(a), it is known that the DCM is subject to abnormal external disturbance under Bragg@5KeV working conditions. In this case, the ability of the hybrid algorithm to suppress uncertain interference is mainly investigated in time range.

The vibration suppression capability of FxLMS-P, FxLMS-PI, and FxLMS-PID hybrid algorithms under Bragg@5KeV working conditions is shown in Fig. 11, from which it can be seen that the FxLMS-based

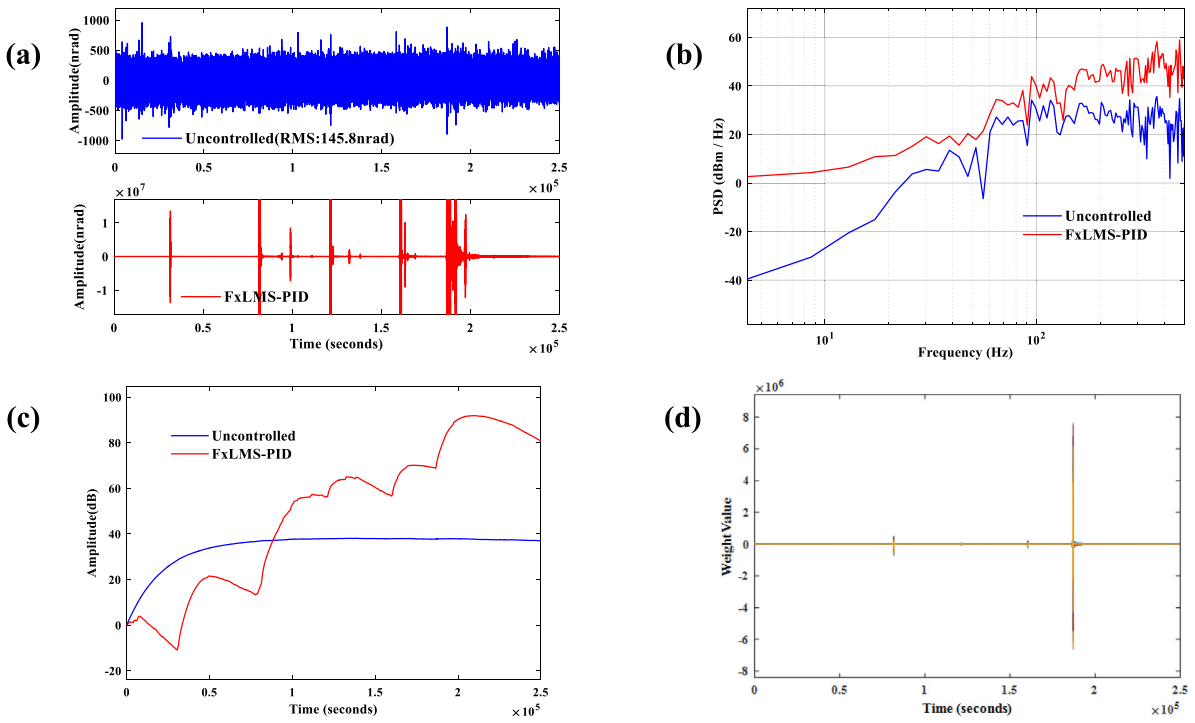

Fig. 7. FxLMS-PID algorithm vibration suppression results. (a) Time-domain results (b) Frequency-domain results (c) Vibration level results (d) Weight iteration results.

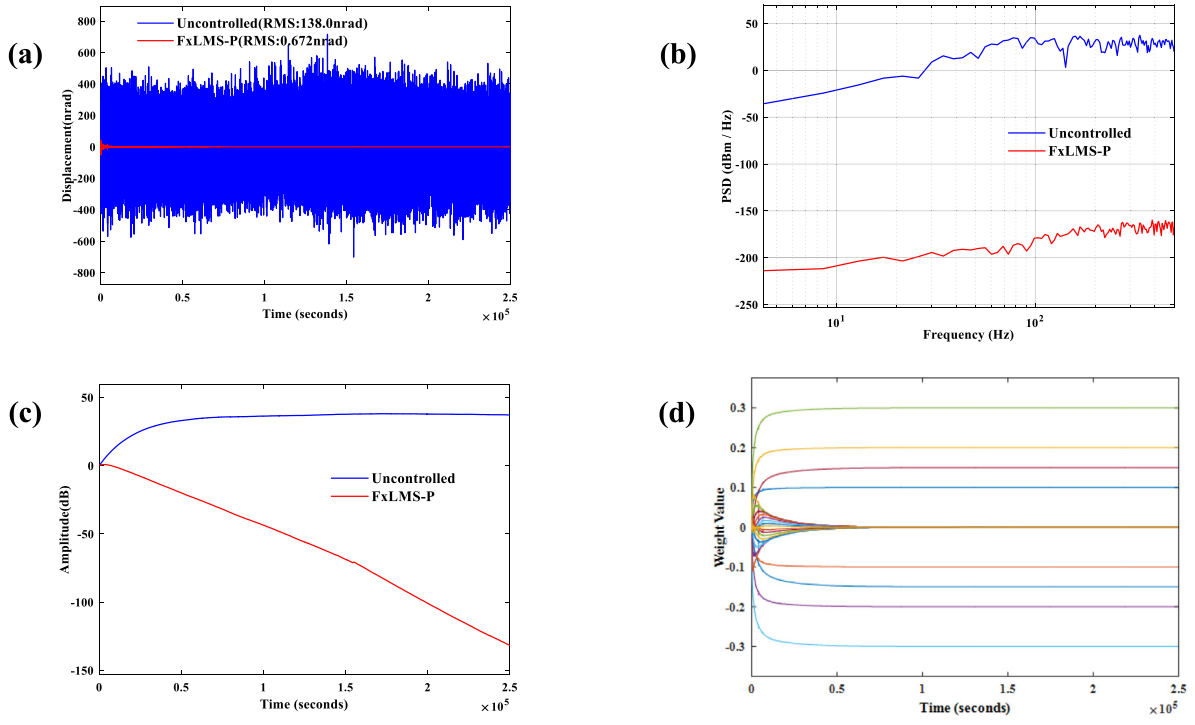

Fig. 8. FxLMS-P algorithm vibration suppression results. (a) Time-domain results (b) Frequency-domain results (c) Vibration level results (d) Weight iteration results.

hybrid algorithm is ineffective. The vibration suppression time-domain results of FxNLMS-P, FxNLMS-PI and FxNLMS-PID hybrid algorithms are shown in Figs. 12–14. As can be seen from the red wireframes in Figs. 12 and 13, the FxNLMS-P and FxNLMS-PI hybrid algorithms cope with the unknown uncertainty perturbations extremely remarkable. However, the FxNLMS-PID hybrid algorithm appears to be non-converging, which has a similar explanation to the case of Fig. 7. The vibration suppression results of FxNLMS-P and FxNLMS-PI hybrid

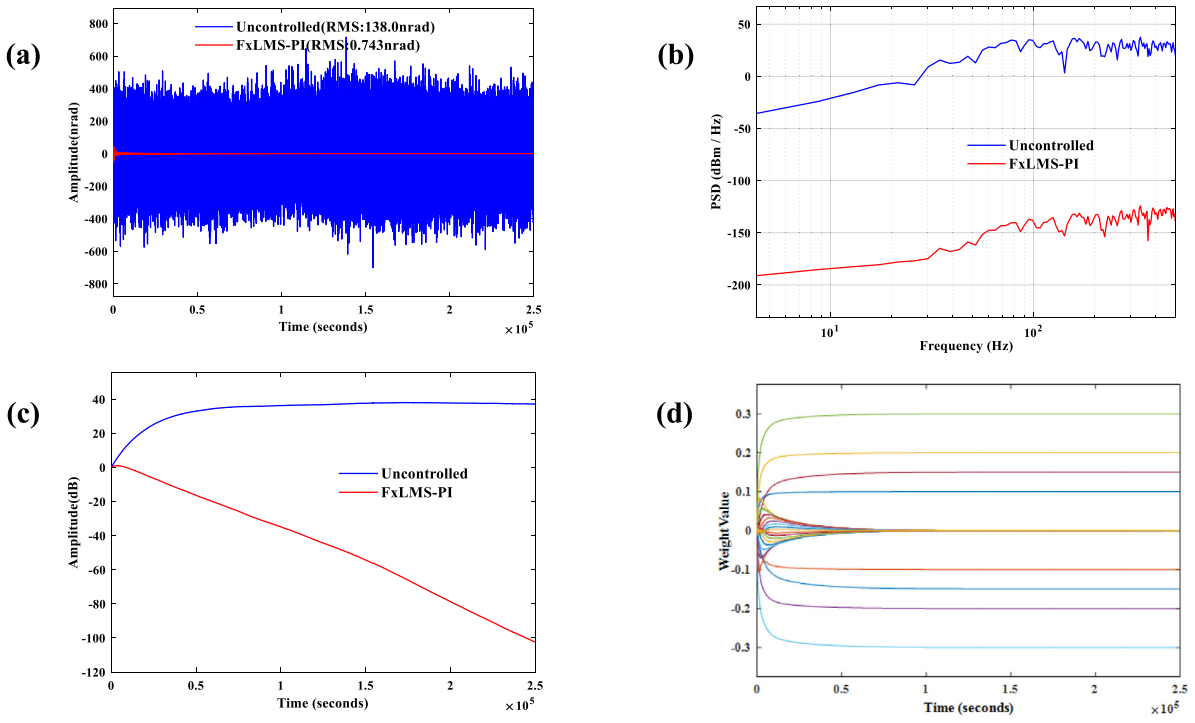

Fig. 9. FxLMS-PI algorithm vibration suppression results. (a) Time-domain results (b) Frequency-domain results (c) Vibration level results (d) Weight iteration results.

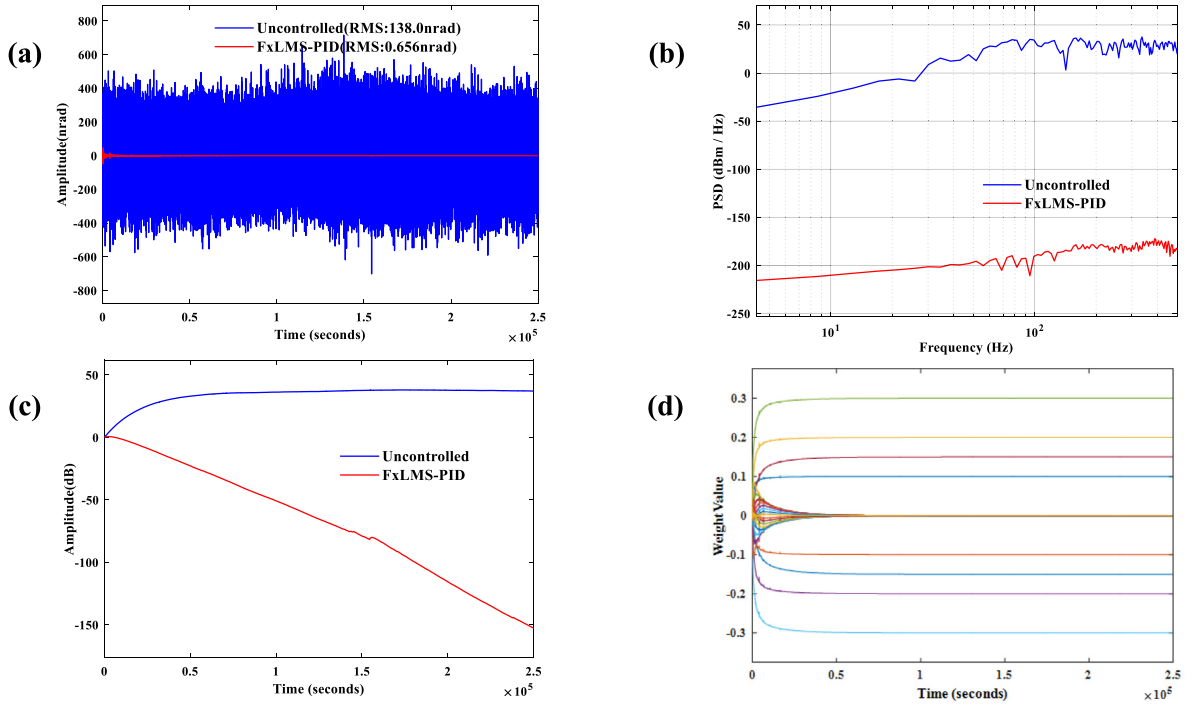

Fig. 10. FxLMS-PID algorithm vibration suppression results. (a) Time-domain results (b) Frequency-domain results (c) Vibration level results (d) Weight iteration results.

algorithm for the green wireframe in Fig. 4(a) are shown in Fig. 15. From Fig. 15, it can be seen that the FxNLMS-P, FxNLMS-PI hybrid algorithm can keep the angular displacement at a considerably low level.

4. Conclusion

This paper mainly verifies the vibration suppression capability of FxLMS-P, FxLMS-PI, and FxLMS-PID algorithms for measured signals

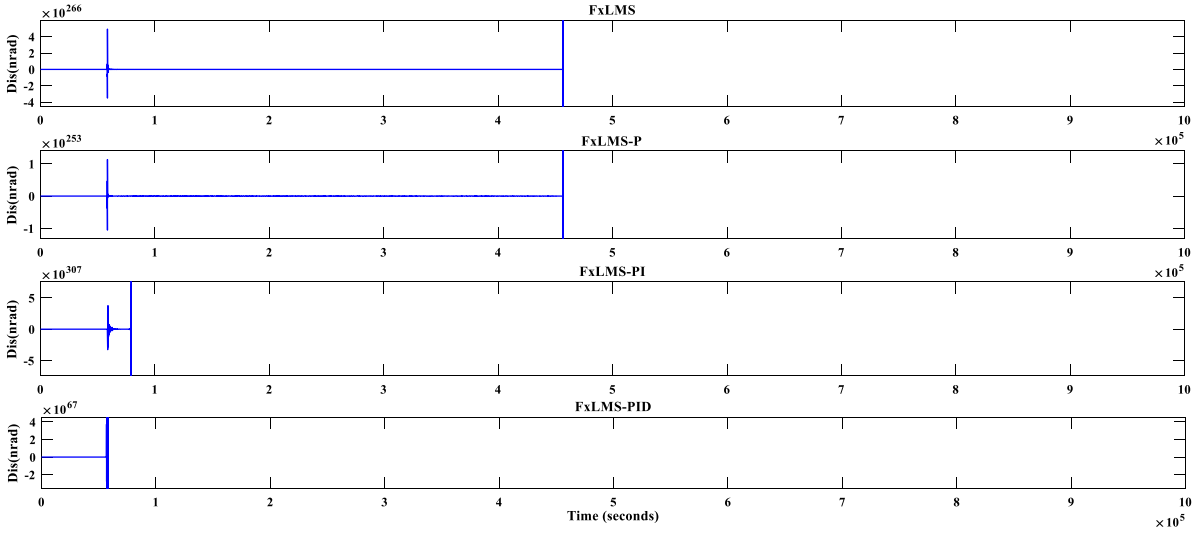

Fig. 11. The results of vibration suppression based on FxLMS hybrid algorithm.

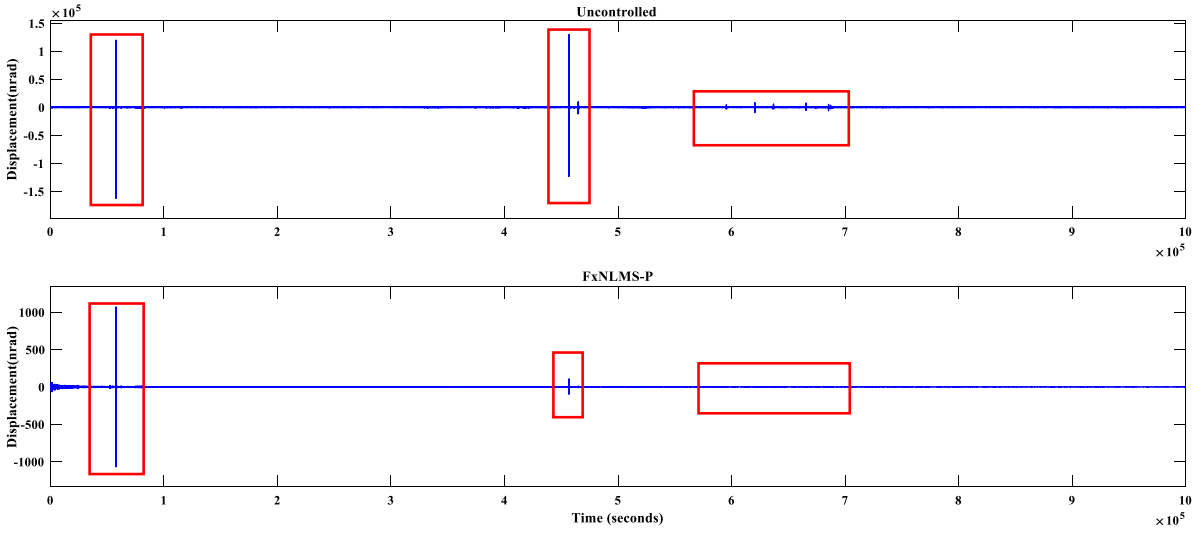

Fig. 12. FxNLMS-P algorithm vibration suppression results.

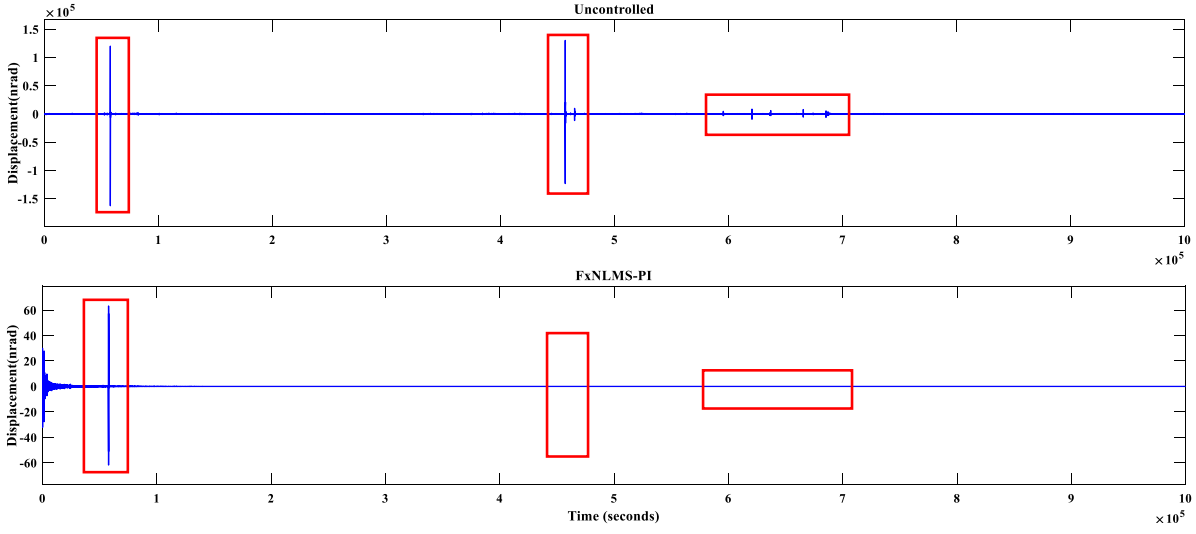

Fig. 13. FxNLMS-PI algorithm vibration suppression results.

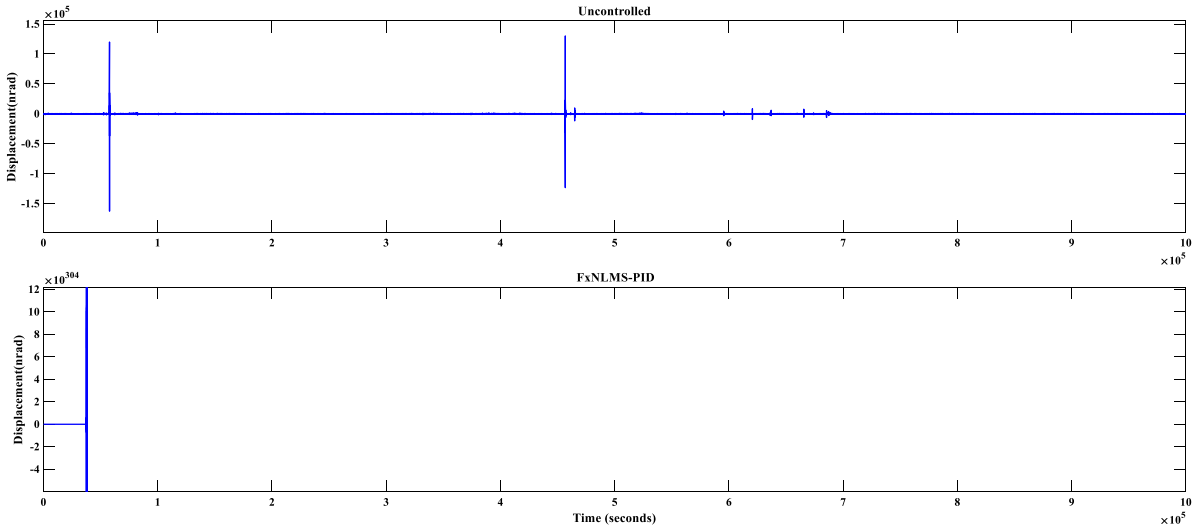

Fig. 14. FxNLMS-PID algorithm vibration suppression results.

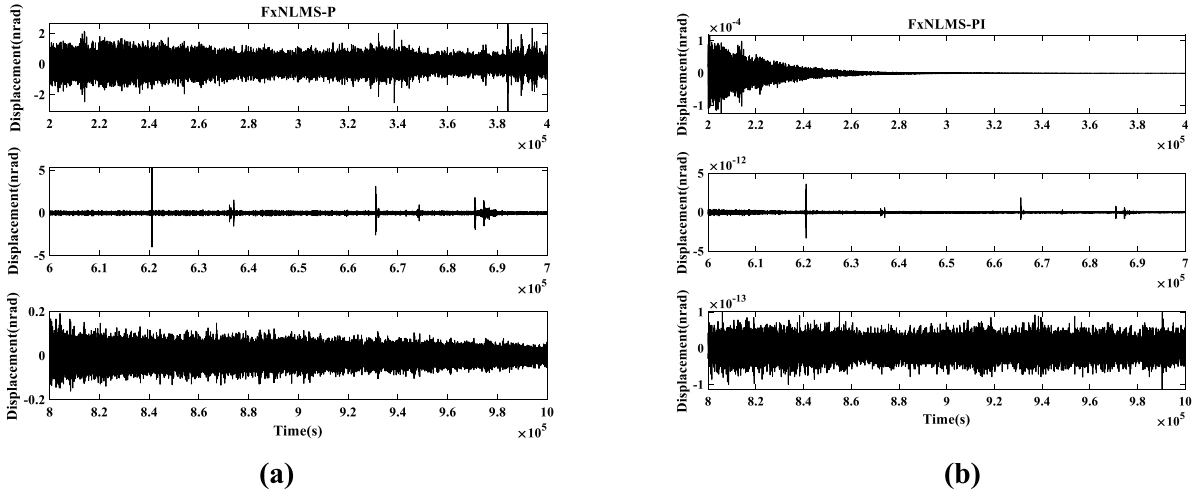

Fig. 15. The vibration suppression results of FxNLMS-P and FxNLMS-PI hybrid algorithm for the green wireframe in Fig. 4(a). (a) FxNLMS-P (b) FxNLMS-PI.

under Bragg@12.66KeV and Bragg@9KeV working conditions and the vibration suppression capability of FxNLMS-P, FxNLMS-PI and FxNLMS-PID algorithms for measured signals under Bragg@5KeV. The results show that the FxLMS/FxNLMS-PI hybrid algorithm has excellent vibration suppression performance and superior ability to cope with unknown anomalous disturbances, which allows the DCM angular displacement to be sustained below 1 nrad in the pitch direction. This work is of great importance for the practical application of key technologies focused on active vibration control to DCM.

Declaration of competing interest

The authors declare that they have no known competing financial interests or personal relationships that could have appeared to influence the work reported in this paper.

Thanks to the support of the researchers at SSRF (Shanghai Synchrotron Radiation Facilities of China).

Data availability

The authors do not have permission to share data.

Acknowledgments

The work is supported by National Natural Science Foundation of China (No. 61974142, No. 62104224) and “Xu-Guang” Talent Program of Changchun Institute of Optics, Fine Mechanics and Physics (CIOMP), China, Chinese Academy of Sciences (CAS) (E01672Y6Q0).

References

[1] P. Willmott, An Introduction to Synchrotron Radiation: Techniques and Applications, John Wiley & Sons, 2019.
[2] Mai Zhenhong, Synchrotron Light Sources and their Applications: The Next Book, Science Press, 2013, In Chinese.
[3] Xu Chaoyin, Synchrotron Radiation Optics and Engineering, University of Science and Technology of China Press, 2013, In Chinese.
[4] M. Yabashi, H. Tanaka, The next ten years of X-ray science, Nat. Photon. 11 (1) (2017) 12, 14.
[5] Ma Lidun, Yang Fujia, Introduction to Synchrotron Radiation Applications, Fudan University Press, 2001, In Chinese.
[6] Choi Jw, Seo Jh, Hwangc, et al., Advanced materials characterization using synchrotron radiation, Curr. Appl. Phys. 30 (2021) 1–3.
[7] Liu Xianyun, Xia Li, Wang Zhengya, et al., Photoionization and photodissociation study of a-pinene using synchrotron radiation, Acta PhotonicaSinica 47 (6) (2018) 0630002.

[8] C.Y. Ren, J.W. Iiang Lkou, Development of micro-laue technique at shanghai synchrotron radiation facility for materials sciences, Sci. China Mater. 64 (9) (2021) 2348–2358.
[9] Yushi Chu, Xinghu Fu, Yanhua Luo, John Canning, Jiaying Wang, Jing Ren, Jianzhong Zhang, Gang-Ding Peng, Additive Manufacturing Fiber Preforms for Structured Silica Fibers with Bismuth and Erbium Dopants. Light: Advanced Manufacturing.
[10] L. Dabin YZhang, D. Martin, et al., The concrete slab studies for the ESRF upgrade beamlines, in: The 7th International Conference on Mechanical Engineering Design of Synchrotron Radiation Equipment and Instrumentation, MEDSI 2012, Shanghai, 2012.
[11] Roland Barrett, et al., New generation mirror systems for the ESRF upgrade beam lines, J. Phys. Conf. Series. (2013).
[12] Noriyuki Igarashi, Kazuyuki Ikuta, Toshinobu Miyoshi, et al., X-ray beam stabilization at BL-17A, the protein micro crystallography beamline of the photon factor, Synchrotron Rad 15 (2008) 292–296.
[13] H. Yamazaki, H. Ohashi, Y. Senba, et al., Improvement in stability of spring-8 X-ray monochromators with cryogenic-cooled silicon crystals, J. Phys. Conf. Ser. (2013).
[14] Hiroshi Yamazaki, et al., Challenges toward 50 nrad-stability of x-rays for a next generation light source by refinements ofspring-8 standard monochromator with cryo- cooled si crystals, in: AIP Conference Proceedings, Vol. 2054, 2019, p. 060018.
[15] Wu Jiaxing, Gong Xuepeng, et al., Improvement of the performance of a cryo-cooled monochromator at SSRF. Part II: Angular stability of the exit beam, Nucl. Inst. Methods Phys. Res. (2021).
[16] Y. Fan, H. Qin, et al., Angular stability measurement of a cooled double-crystal monochromator at SSRF, Nucl. Instrum. Methods Phys. Res. Section Accel. Spectrom. Detect. Assoc. Equip. 983 (2020) 164636.
[17] J. Qiu, M. Haraguchi, Vibration control of a plate using a self-sensing piezoelectric actuator and an adaptive control approach, J. Intell. Mater. Syst. Struct. 17 (8–9) (2006) 661–669.
[18] Yuan H Guan, Teik C Limb, W Steve Shepard Jr., Experimental study on active vibration control of a gearbox system, J. Sound Vib. 282 (2005) 713–733.
[19] Yuan H Guan, Mingfeng Li, Teik C. Lim, W Steve Shepard Jr., Comparative analysis of actuator concepts for active gear pair vibration control, J. Sound Vib. 269 (2004) 273–294.
[20] Mingfeng Li, Teik C Lim, Actuator design and experimental validation for active gearbox vibration control, Smart Mater. Struct. 15 (2006) 1–6.
[21] Yuan H Guan, W Steve Shepard Jr., Teik C. Lim, Mingfeng Li., Experimental study on active gear mesh vibration control, Smart Struct. Mater. 5383 (2004) 366–375.
[22] Mingfeng Li, Active Vibration Control of a Gearbox System with Emphasis on Gear Whine Reduction, A dissertation submitted to the division of research and advanced studies of the University of Cincinnati, 2005.
[23] Mingfeng Li, Teik C Lim, W Steve Shepard Jr., Modeling active vibration control of a geared rotor system, Smart Mater. Struct. 13 (2004) 449–458.
[24] R.H. Kwong, E.W. Johnson, A variable step size LMS algorithm, IEEE Trans. Signal Process. 40 (7) (1992) 1633–1642P.
[25] V.J. Mathews, Z. Xie, A stochastic gradient adaptive filter with gradient adaptive step size, IEEE Trans. Signal Proc. 41 (6) (1993) 2075–2087P.
[26] T. Aboulnasr, K. Mayyas, A robust variable step-size LMS-type algorithm: analysis and simulations, IEEE Trans. Signal Proc. 45 (3) (1997) 631–639P.
[27] D.I. Pazaitis, A.G. Constantinides, A novel Kurtosis driven variable step-size adaptive algorithm, IEEE Trans. Signal Proc. 47 (3) (1999) 864–872P.
[28] A. Mader, H. Puder, G.U. Schmidt, Step-size control for acoustic echo cancellation filters: an overview, Signal Proc. 80 (2000) 1697–1719P.
[29] W. Ang, B. Farhang-Boroujeny, A new class of gradient adaptive step-size LMS algorithms, IEEE Trans. Signal Proc. 49 (4) (2001) 805–810P.
[30] H.C. Shin, A.H. Sayed, W.J. Song, Variable step-size NLMS and affine projection algorithms, IEEE Signal Proc. Lett. I 1 (2) (2004) I32–135P.
[31] L.J. Eriksson, Development of the filtered-U algorithm for active noise control, J. Acoust. Soc. Am. 89 (1) (1991) 257–265.
[32] K. Mayyas, Avariable step-size selective partial update LMS algorithm, Digit. Signal Process. 23 (1) (2013) 75–85.
[33] Dariusz Bismor, Simulations of partial update LMS algorithms in application to active noise control, in: The International Conference on Computational Science, in: ICCS 2016.
[34] Ho-Wuk Kim, et al., Modified-filtered-u LMS algorithm for active noise control and its application to a short acoustic duct, Mech. Syst. Signal Process. 25 (2011) 475–484.
[35] Lingbo Xie, et al., Vibration control of a flexible clamped-clamped plate based on an improved FULMS algorithm and laser displacement measurement, Mech. Syst. Signal Process. 25 (2011) 475–484.
[36] Amrita Puri, et al., Modal filtered-x LMS algorithm for global active noise control in a vibro-acoustic cavity, Mech. Syst. Signal Process. 110 (2018) 540–555.
[37] Philipp Zech, et al., Active control of planetary gearbox vibration using phase-exact and narrowband simultaneous equations adaptation without explicitly identified secondary path models, Mech. Syst. Signal Process. 120 (2019) 234–251.
[38] Y.S. Wang, et al., Active control for vehicle interior noise based on DWT-FxLMS algorithm using a piezoelectric feedback system, Appl. Acoust. 167 (2020) 107–409.
[39] Lei. Luo, et al., A novel acoustic feedback compensation filter for nonlinear active noise control system, Mech. Syst. Signal Process. 158 (2021) 107675.